190 GHz Bandwidth Modified Uni-Traveling Carrier Photodiodes with High Saturation Power

Yuxin Tian[1], Bing Xiong[1*], Changzheng Sun[1], Zhibiao Hao[1], Jian Wang[1], Lai Wang[1], Yanjun Han[1,2], Hongtao Li[1], Lin Gan[1], and Yi Luo[1,2]

[1] Beijing National Research Center for Information Science and Technology (BNRist), Department of Electronic Engineering, Tsinghua University, Beijing 100084, China

[2]Flexible Intelligent Optoelectronic Device and Technology Center, Institute of Flexible Electronics Technology of THU, Jiaxing 314000, Zhejiang, China

E-mail: bxiong@mail.tsinghua.edu.cn

Abstract: Back-illuminated modified uni-traveling carrier photodiodes with improved saturation performance at ultra-high frequencies are developed. The 4-µm-diameter PD exhibits a 3-dB bandwidth of 190 GHz with a saturation power of −1.21 dBm@190 GHz. © 2022 The Author(s)

1. Introduction

Photonic-based technologies have become increasingly essential for millimeter-wave signal generation due to the advantages of broad bandwidth, high output power and compact size, which have been widely employed in radar technology, sub-THz wireless communications, and mm-wave/THz high-resolution imaging [1-3]. Photodiodes (PDs) serve as a key component in such applications. Uni-traveling carrier photodiodes (UTC-PDs) are particularly attractive, as they exhibit both wide bandwidth and high output power. For instance, 2×10 μm^2 waveguide UTC-PDs demonstrate a 3-dB bandwidth of 170 GHz, and an output power about −9 dBm at 200 GHz [4]. Flip-chip bonded 4-µm-diameter modified UTC-PDs exhibit a 3-dB bandwidth up to 120 GHz as well as an unsaturated RF output power of –8.5 dBm at 160 GHz [5]. In our previous work, 4.5-µm-diameter photodiodes with a 3-dB bandwidth of 156 GHz and a saturation RF power of –0.53 dBm at 170 GHz are demonstrated [6]. However, PDs with both ultra-wide bandwidth over 200 GHz and high output power remain a challenge.

In this work, we extend the RC-limited bandwidth of the PD by increasing the depletion region thickness to reduce device capacitance, while reducing the contact resistance of the device with reduced active area. Meanwhile, a gradient doped thin absorption layer and a cliff layer with optimized doping level are adopted to improve saturation performance at ultra-high frequencies. The fabricated 4-µm-diameter modified uni-traveling carrier photodiode (MUTC-PD) exhibits an extremely high bandwidth of 190 GHz, together with a high saturation output power of −1.21 dBm at 190 GHz.

2. Design of Device Structure

The bandwidth of a 4.5-µm-diameter MUTC-PD reported in our previous work [6] is RC limited, in which the InP depletion layer is only 120 nm. According to Fig. 2(a), as the InP depletion region thickness increases, the RC-limited bandwidth also increases due to the reduced junction capacitance, while the transit-time limited bandwidth decreases as a result of increased transit time for electrons. The maximum 3-dB bandwidth of 213 GHz is obtained with an InP depletion layer thickness of 200 nm. To further improve the 3-dB bandwidth, the active area of the PD is scaled down to reduce device capacitance. As shown in Fig. 1(b), the RC-limited and the transit-time limited bandwidths are similar for a 4-µm-diameter PD, and a 3-dB bandwidth of 230 GHz is expected. However, bandwidth improvement by scaling down the active area of the PD assumes constant contact resistance. In practice, active area reduction leads to increased ohmic contact resistance, which reduces the RC-limited bandwidth of the 4-µm-diameter PD from 307 GHz to 289 GHz. To reduce the contact resistance of PDs, we optimized the Pt interlayer thickness in the Ti/Pt/Au electrode on the p^+-InGaAs contact layer and the annealing temperature to minimize the contact resistivity. A low contact resistivity is achieved with Ti(20nm)/Pt(60nm)/Au(200nm) p-electrode annealed at 350℃ for 1 min.

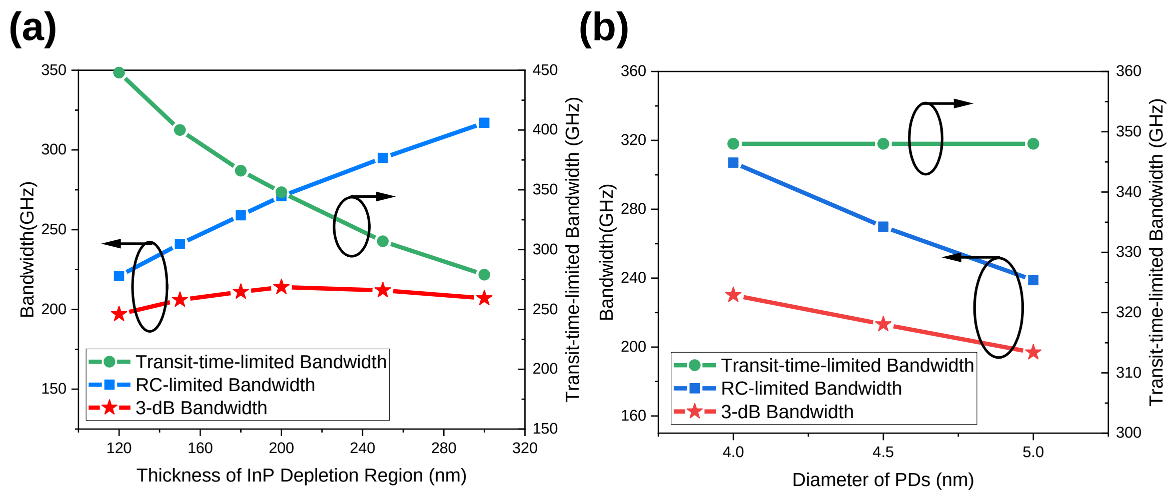

Fig. 1. Variation of the PD bandwidth with (a) the InP depletion region thickness and (b) the device diameter.

The doping profiles of both the absorption layer and the cliff layer are also carefully investigated. By adopting a gradient doped thin absorption layer and a cliff layer with optimized well-chosen doping concentration, the electric field in the depleted InGaAs absorption layer is enhanced, thus making the PD less susceptible to the space charge effect. Meanwhile, the electric field in the depleted InP layer is reduced to the range for electron velocity overshoot [7], thus avoiding electron accumulation. As a result, the PD exhibit improved saturation performance. Figures 2(a) and 2(b) show the simulated electric field distribution in 4-μm-diameter MUTC-PDs with n-doped cliff layer of 1×10^{17} cm^{-3} and 3×10^{17} cm^{-3}, respectively. As shown in Fig. 2(a), for the PD with a cliff layer doping level of 1×10^{17} cm^{-3}, the same as in our previous work [6], the electric field becomes screened in the depleted absorption region, as indicated by the yellow shade. When the photocurrent increases to 7.5 mA, the electric field is reduced to almost zero in the absorption region, which slows down the electron drift process and limits the maximum output power. On the other hand, as shown in Fig. 2(b), for the PD with a cliff layer doping level of 3×10^{17} cm^{-3}, the electric field in absorption region is strengthened, and screening occurs only at the junction between the depleted absorption region and the InP depletion layer, as indicated by the green shade. As a result, saturation current is increased to 9.5 mA. As the photocurrent increases, the collection layer becomes non-depleted, and the junction capacitance increases. According to Fig. 2(c), the simulated peak RF output power of the designed epitaxy structure is about 0.3 dBm, corresponding to a saturation photocurrent of 9.3 mA.

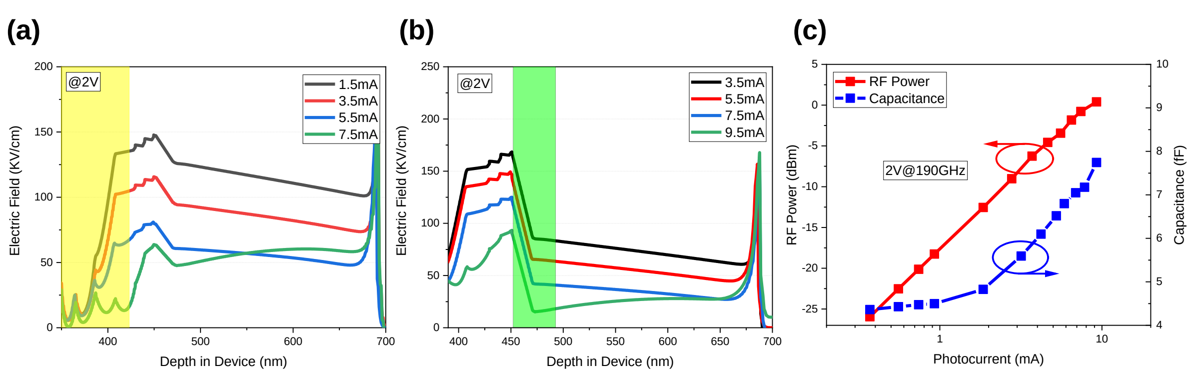

Fig. 2. Electric field distributions in depletion region of 4-μm-diameter PDs with different cliff layer doping concentrations: (a) 1×10^{17} cm^{-3} and (b) 1×10^{17} cm^{-3}. (c) Simulated RF power and capacitance versus photocurrent.

3. Experiment Results

The I-V characteristics of the fabricated MUTC-PDs are shown in Fig. 3(a). The dark current for the 4-μm diameter PD is only 4.13 nA at 2 V reverse bias, and the measured series resistance is 17 Ω, which is reduced from 20 Ω. An optical heterodyne system is used to measure its frequency response. Three different MMW power sensor heads are employed to cover the frequency range from dc to 50 GHz, V-band (50-75 GHz) and W-band (75-110 GHz), respectively, and the insertion losses of the coaxial cables and the waveguide probes are carefully calibrated out. As for frequencies above 110 GHz, a VDI-Erickson power meter (PM5B) is used to record the RF power. The loss of the GGB probe, a WR10-WR8 waveguide taper, and a WR10-WR5.1 waveguide taper are calibrated out. The frequency response tested under 5 mA and 6.5 mA with a fixed reverse bias of 2 V are plotted in Fig. 3(b). The PDs exhibits an ultrafast performance with 3-dB bandwidth of 190 GHz at 6.5 mA. The output RF power versus photocurrent of the 4-μm-diameter MUTC-PD at 190 GHz with 2 V reverse bias is plotted in Fig. 3(c). The photocurrent at 1-dB compression is 9 mA, corresponding to a high output power of –1.21 dBm at 190 GHz, which is in good agreement with the simulation.

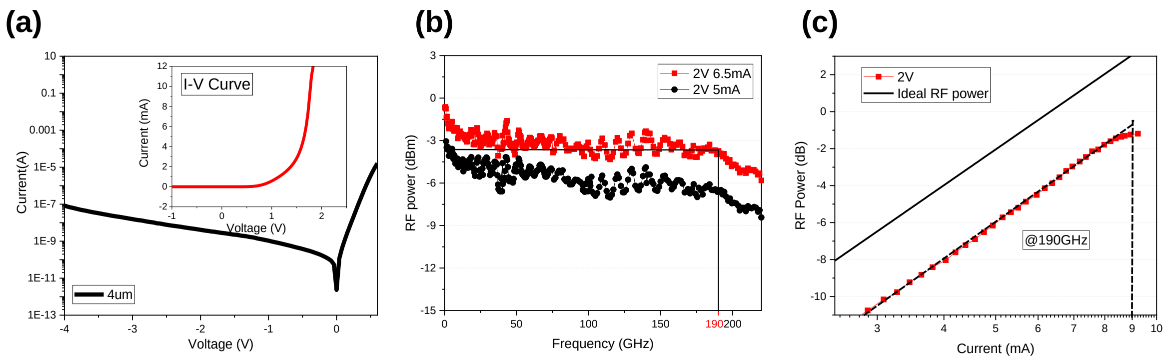

Fig. 3. (a) I-V characteristics of the fabricated PD. (b) Measured frequency responses of a 4-μm diameter PD (c) RF power versus photocurrent at 190 GHz.

5. Conclusion

In this work, we propose thick depletion region to alleviate RC charging time, Meanwhile, scaled down active area with low contact resistivity is demonstrated to further improve the RC-limited bandwidth. A gradient doped thin absorption and an optimized cliff layer are adopted to improve the saturation performance of the MUTC-PD at ultra-high frequencies. The fabricated 4-μm-diameter PD exhibits a 3-dB bandwidth of 190 GHz and a saturation output power of –1.21 dBm at 190 GHz.

Acknowledgements

This work was supported in part by National Key R&D Program of China (2021YFB2800604); National Natural Science Foundation of China (62235005, 61975093, 61927811, 61991443, 61822404, 61974080, 61904093, and 61875104); Key Lab Program of BNRist (BNR2019ZS01005); Collaborative Innovation Centre of Solid-State Lighting and Energy-Saving Electronics.

References

[1] N. Paik, N. Sastry, and I. SantiPrabha, "Effectiveness of noise jamming with White Gaussian Noise and phase noise in amplitude comparison monopulse radar receivers." In 2014 IEEE International Conference on Electronics, Computing and Communication Technologies (CONECCT), 1-5 (2014).
[2] C. Shahriar, M. La Pan, and M. Lichtman, “PHY-layer resiliency in OFDM communications: A tutorial.” IEEE Communications Surveys & Tutorials, 17, 292-314 (2014).
[3] T. Nagatsuma, T. Kumashiro, Y. Fujimoto, K. Taniguchi, K. Ajito and Y. Kado, “Millimeter-wave imaging using photonics-based noise source.” In 2009 34th International Conference on Infrared, Millimeter, and Terahertz Waves, 1-2 (2009).
[4] E. Rouvalis, M. Chtioui, C. C. Renaud and A. J. Seeds, “170 GHz uni-traveling carrier photodiodes for InP-based photonic integrated circuits.” Optics express, 20, 20090-20095 (2012).
[5] J. S. Morgan, K. Sun, Q. Li, S. Estrella and A. Beling, “High-power flip-chip bonded modified uni-traveling carrier photodiodes with− 2.6 dBm RF output power at 160 GHz.” 2018 IEEE Photonics Conference, 1-2 (2018).
[6] E. Chao, B. Xiong, C. Sun and Y. Luo, “D-Band MUTC Photodiodes with Flat Frequency Response.” IEEE Journal of Selected Topics in Quantum Electronics, 28, no.3802208 (2021).
[7] T. J. Maloney and J. Frey, “Transient and steady-state electron transport properties of GaAs and InP.” Journal of Applied Physics, 48, 781-787 (1997).